Density of the Lunar Surface

Abstract. *The evidence that the lunar soil is basaltic permits a closer estimate of its density from the radiothermal and radar data. The mean density at the surface is 0.6 ± 0.2 gram per cubic centimeter, increasing to 1.0 gram per cubic centimeter at a depth of a few centimeters; still higher densities at depths of up to meters are implied by the radar observations.*

Now that the Surveyor V experiment in chemical analysis has established (*1*) that part of the lunar surface has a composition resembling basalt, it is interesting to use the measured electrical properties of basalt, in conjunction with the lunar radar and radiothermal observations, to refine the estimates of the density of the surface layers.

Measurements in this laboratory on solid basalt at wavelengths of 68 cm and 8.6 mm have shown that the dielectric constant is almost independent of frequency. Furthermore, when these data were used to calculate the dielectric constant of powdered basalt, by use of the expression of Twersky (*2*), the results were almost independent of the source and variety of basalt; the sample-to-sample variations among our ten specimens of basalt from four sources produced an overall range of only ± 9 percent in our estimates of density. We have confirmed the validity of Twersky's expression by measurements on powdered basalt and other rocks.

It is well known that the lunar radar observations, interpreted as reflections from a rough, homogeneous, dielectric sphere, yield values for the dielectric constant that are significantly higher than those determined from Moon's radiothermal emission. This discrepancy has been discussed (*3*) in terms of a two-layer model, with a discrete increase in the dielectric constant at a depth that is small compared to an absorption length—a condition readily met in basalt powder—but that may be comparable to a wavelength. Other authors have considered models in which the dielectric constant increases linearly (*4*) or exponentially (*5*) with depth; always it was found that the radar reflectivity is augmented above the reflectivity due to the topmost, low-density layer, although it never reaches as high a value as would obtain if the deeper layers were exposed directly.

By contrast the radiothermal observations, especially when made by the polarization method on regions close to the limb, are a measure of the dielectric constant of the material at the surface. In particular, for a material whose dielectric constant is changing only slowly with depth, it is the topmost quarter-wavelength that principally determines the ratio of the polarized intensities.

By measuring these intensities, Soboleva (*6*) found a radiothermal dielectric constant of 1.65 at 3.2-cm wavelength, and Heiles and Drake (*7*) determined 2.1 at 21 cm. In powdered basalt these values are obtained at densities of 0.63 ± 0.14 and 1.0 ± 0.2 g/cm^3, respectively, where the errors correspond only to the limits quoted by these authors. We infer that the uppermost centimeter of the lunar surface has a typical density of 0.6 g/cm^3, which increases to 1.0 g/cm^3 over the next few centimeters, corresponding to powders about 25- and 35-percent solid.

These estimates agree closely with those made by Jaffe (*8*) from the landing dynamics at the Surveyor I site; they are consistent with the Surveyor III estimates of Christensen *et al.* (*9*), but not with the density of 1.5 g/cm^3 adopted by Scott *et al.* (*10*) for average mare material.

The absorption length in powdered basalt of these porosities is about 50 wavelengths—approximately 2 m for a wavelength of 3.6 cm and 30 m for a wavelength of 68 cm, where Evans and Hagfors (*11*) have measured radar reflectivities corresponding to dielectric constants of 2.72 and 2.79, respectively. The fact that these are significantly higher than the radiothermal determinations suggests that the density increases still further after the first 5 cm, although probably not very rapidly at depths greater than 1 to 2 m. On Evans' (*3*) model, the dielectric constant at this depth is intermediate between those of highly compressed powder (about 3 at a porosity of 40 percent) and solid basalt (about 8). A two-layer model, by neglect of slow changes in dielectric constant, tends to overestimate the density in the deeper layer, and we interpret the radar results as showing that the basalt is still powdered, although of almost minimum porosity, at depths of a few meters.

MALCOLM J. CAMPBELL
JURIS ULRICHS, T. GOLD
Center for Radiophysics and Space Research, Cornell University, Ithaca, New York 14850

References and Notes

1. A. L. Turkevitch, E. J. Franzgrote, J. H. Patterson, *Science* **158**, 635 (1967).
2. V. Twersky, *J. Math. Phys.* **3**, 724 (1962).
3. J. V. Evans, *J. Res. Nat. Bur. Std.* **69D**, 1637 (1965).
4. A. Giraud, *ibid.*, p. 1677.
5. Y. G. Matveev, *Astron. Zh.* **44**, 419 (1967).
6. N. S. Soboleva, *ibid.* **39**, 1124 (1962).
7. C. E. Heiles and F. D. Drake, *Icarus* **2**, 281 (1963).
8. L. D. Jaffe, *J. Geophys. Res.* **72**, 1727 (1967).
9. E. M. Christensen *et al.*, in *Surveyor 3 JPL Project Doc. 125* (15 May 1967), sect. 4.
10. R. F. Scott, F. I. Roberson, M. C. Clary, *ibid.*, sect. 5.
11. J. V. Evans and T. Hagfors, *Icarus* **3**, 151 (1964).
12. Supported by NASA grant NsG-382.

20 November 1967

X-ray Diffraction: New High-Speed Technique Based on X-ray Spectrography

Abstract. *A method has been developed for obtaining lattice spacings of powder samples by x-ray diffraction in times potentially as short as 1 second. The sample is irradiated with polychromatic radiation from an x-ray tube, and the energy spectrum of x-rays scattered at a given angle is observed with a semiconductor radiation detector, coupled with a pulse-height analyzer.*

The condition for the diffraction of x-rays by a crystal lattice can be expressed in the form of Bragg's law:

$$2d(hkl) \cdot \sin \theta = \lambda \qquad (1)$$

where $d(hkl)$ is the interplanar spacing of reflecting planes with the indices hkl, θ is the glancing angle of incidence on the plane (hkl), and λ is the wavelength of the radiation used. It is generally applied to polycrystalline materials by use of the powder method of Debye and Scherrer and of Hull. Monochromatic radiation, normally K_α radiation of the tube anode material, is used, making λ equal to λ_{K_α}. The d spacings are derived from the observed θ values corresponding to diffraction maxima. The diffraction condition can be interpreted very simply by use of a reciprocal lattice construction (*1*).

If direct recording techniques, such as a diffractometer with a proportional or scintillation counter, are to be used, the scanning rate cannot exceed a certain limit set by the receiving slit width and the required signal-to-noise ratio. Thus, with conventional x-ray diffraction equipment, an angular range of $2\theta = 120$ deg can be recorded in less than about 1 hour only with some loss of resolution. If times available for observation are much shorter, image-amplification techniques or other diffraction methods (such as electron diffraction) must be used. In the case of rapid transformations of metastable alloy phases now under study (*2*), electron diffraction was difficult to use; a faster x-ray diffraction method was desired.

The polychromatic ("white") component of the x-radiation used in diffraction contributes to the continuous background of the diffraction pattern, along with inelastic scattering by the sample, fluorescence, and so on. The white component of the incident radiation undergoes coherent scattering (diffraction) by each crystal of the powder or sheet sample. Therefore the radiation scattered in any given direction contains information about the lattice, which is yielded by spectral analysis of the diffracted beam; with the aid of high-resolution semiconductor detectors, this analysis can be performed very quickly.

We combined a diffractometer having a Siemens x-ray source (Fe anode with 8 ma at 45 kv) with a lithium-drifted Si [Si(Li)] semiconductor detector connected to a 4096-channel pulse-height analyzer; use of such detectors for spectrography of *K* and *L* emission lines has been described (*3*).

The detection system included a TMC low-energy photon spectrometer (*4*) consisting of a Si(Li) detector (30 mm^2 by 3 mm) and a field-effect transistor preamplifier. The detector and the field-effect transistors were cooled in a liquid-nitrogen cryostat. Pulses from the preamplifier were passed through a Tennelec TC-200 amplifier before being analyzed and stored in a Packard 4096-channel pulse-height analyzer. The amplifier gain was adjusted so that the energy region between 0 and 64 kev was spread over a 1024-channel quadrant of the analyzer memory. The pulse-height-versus-energy curve (essentially linear) of the system was determined from spectra taken with standard sources of ^{57}Co and ^{241}Am (*3*); the full width at half-maximum (FWHM) of photopeaks produced by the standards varied from about 0.60 to 0.83 kev over the range 14 to 60 kev.

The geometric relation of source, diffracting sample, and detector was identical with that used in standard diffraction experiments, with the line normal to the specimen bisecting the angle (180 deg $-$ 2θ) between the incident and diffracted beams. The diffractometer was set to a predetermined low angle (see below), and counts were taken for various periods with sheet samples of Cu, Ag, Re, Pt, and Au.

Figure 1a shows a diffraction pattern of Pt sheet; all diffraction peaks up to (333/511) are present and resolvable, and the Pt *L*-radiation is resolved into α, β, and γ peaks. The similarity to a conventional powder diffraction pattern of a face-centered-cubic (fcc) material is immediately obvious if one considers a slight (100)[001] cube texture of the Pt sheet, which enhances the (200) and (400) reflections. The FWHM values of the peaks (Fig. 1a) are slightly greater than the values quoted above because of the contribution of slit width in the case of diffraction peaks and because of multiple components for the fluorescence peaks.

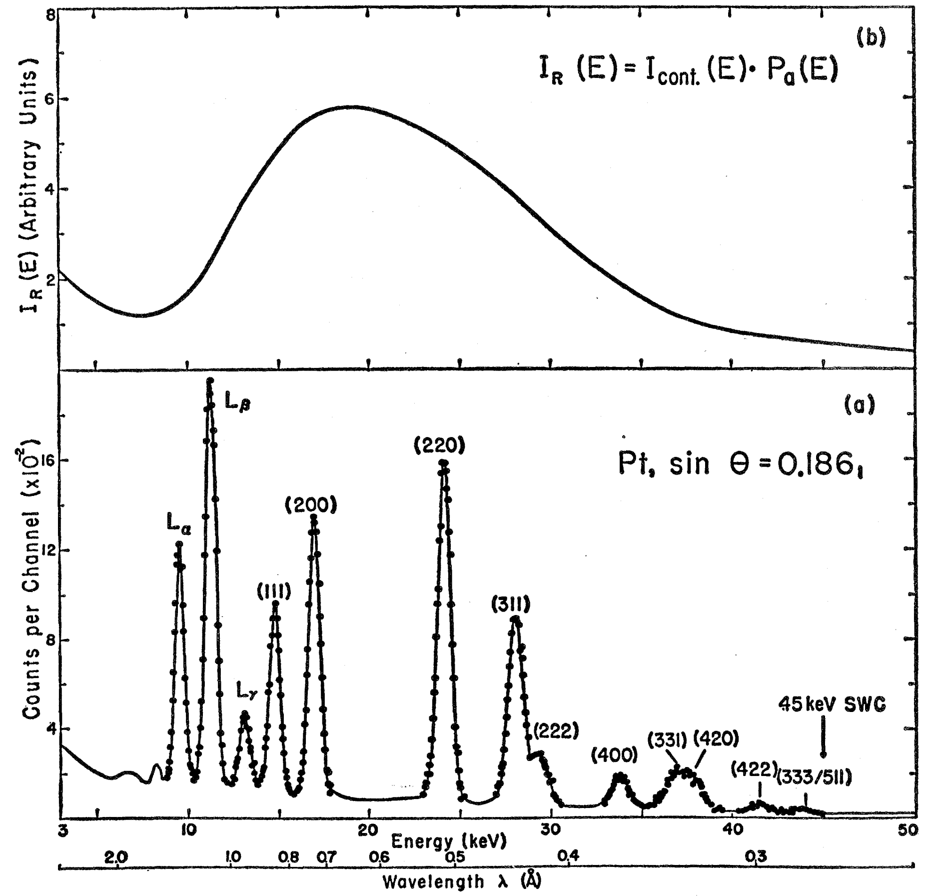

Fig. 1. (a) Diffraction pattern and *L*-fluorescence spectrum of platinum sheet, obtained by x-ray spectroscopy; *SWC*, shortwave cutoff of x-ray beam. (b) Response of detector to undiffracted polychromatic x-ray beam.

The upper curve (Fig. 1b) represents the response of the detector to the undiffracted primary beam. The observed response function $I_R(E)$ is determined by two factors:

$$I_R(E) = I_{\text{cont}}(E) \cdot P_a(E) \qquad (2)$$

where $I_{\text{cont}}(E)$ is the intensity of emitted white radiation of energy E, and $P_a(E)$ is the probability of photopeak absorption of photons of energy E by the detector. One sees that $I_R(E)$ has a maximum at about $E = 19$ kev and falls off rapidly at lower energies [because of reduction in $I_{\text{cont}}(E)$ and $P_a(E)$, in the latter because of such factors as absorption in the cryostat window] and at higher energies [because of reduction in $P_a(E)$]. Note that in Fig. 1b the high-energy tail of the $I_R(E)$ distribution extends above the cutoff of the x-ray tube (45 kev) because of some pileup of pulses as a result of the high count rate from the direct beam; this effect is not present in the diffraction patterns, which were taken at much lower count rates.

The shape of $I_R(E)$ is superimposed over the diffraction pattern given by the customary x-ray crystallographic treatment; the shape of $I_R(E)$ causes the low intensity of the high-energy lines, especially (422) and (333/511), prior to the high-energy cutoff at 45 kev.

For evaluation of the *d*-spacings from

the diffraction pattern (Fig. 1a), Bragg's law is best rewritten in terms of photon energy E:

$$E = hc/\lambda = 12.398/\lambda \qquad (3)$$

if E is expressed in kiloelectron volts and λ is in angstroms, which leads to

$$d(hkl) = (6.199/\sin\theta)\cdot(1/E) \qquad (4a)$$

or

$$|\mathbf{k}| = 1/d = (\sin\theta/6.199)\,E \qquad (4b)$$

This form demonstrates clearly the proportionality of the magnitude $|\mathbf{k}|$ of the reciprocal lattice vector to the energy E of the diffraction peak.

In this experiment the uncertainty of determination of the lattice parameter a_0 is about 0.18 percent. The fractional error, $\Delta d/d$, equals $\Delta E/E$ after errors in θ are minimized by proper alignment of the diffractometer. Although the FWHM of the photopeaks is about 0.7 kev, centroids of the peaks can be determined within 0.1 kev over the entire energy range. Thus the most accurate determinations of a_0 are those based on d-values from the diffraction peaks observed at the highest energies: for example, $\Delta d/d$ for the (422) and (333/511) reflections is about $0.1/40 = 0.25$ percent.

Combination of information from both these peaks drops the uncertainty to 0.18 percent, which corresponds to $\Delta a_0 = 0.007$ Å for Pt. While this error value is about ten times that obtainable with a conventional lattice-parameter determination of fair quality, it can be significantly improved by use of more reflections and by shifting of the diffraction pattern to higher energies by suitable choice of sin θ. The shift can be achieved with a higher tube voltage and by use of a Ge(Li) detector rather than the Si(Li) detector, with resultant decrease in $\Delta E/E$ by a factor of at least 2; this decrease is possible because $P_a(E)$ does not decrease as fast, with increase in E, for Ge as for Si (*3*). Appropriate choice of sin θ also is needed to avoid superimposition of the fluorescent radiation excited in the sample or target, or both, over important parts of the diffraction pattern.

Although the pattern in Fig. 1a was obtained by counting for 1.5 hours to give good statistics, fair patterns of all materials named above were obtained with 5- to 10-minute exposures. These materials include Re, which is hcp (A3 type) and thus yields a diffraction pattern with more-closely spaced lines than those of the fcc (A1-type) metals. The first 13 lines up to (203) (which occurred at 33.4 kev for the chosen sin θ setting) were resolved or clearly detectable. By taking all available values into account we obtained an axial ratio $c{:}a = 1.617 \pm 0.003$, in excellent agreement with the literature value, $c{:}a = 1.615_4$ (*5*).

Compared to the conventional x-ray powder diffraction technique, the new method, which may be suitably termed powder-diffraction spectrography, gathers information about the reciprocal lattice at a rate greater by two to three orders of magnitude; thus very short observation times are possible, especially with certain experimental modifications. The present arrangement yielded recognizable diffraction patterns in 15 seconds; by use of a W-target tube, with higher emission and a correspondingly higher tube voltage and current, the intensity $I_{\text{cont}}(E)$ may be easily increased by a factor of 10. Use of a rotating anode tube with about 6 kw may further shorten the time by a factor of 5. As we have noted $P_a(E)$ can be increased at higher energies by use of Ge(Li) instead of Si(Li) for the detector. With these improvements, recognizable diffraction patterns are probably possible within 0.3 second; such brief exposure is valuable during transient or extreme conditions such as the rapid transformation of metastable phases or very high pressures. In order to follow rapid transitions one must take successive spectra; this we did by storing the spectra in the various quadrants of the analyzer memory or by recording them on magnetic tape.

The new method may be especially applicable for x-ray determinations of crystal structures under high pressure for another reason: only one beam-exit port is required, which can be chosen at a convenient angle θ, rather than a port permitting the range of θ values that is necessary in the conventional powder method. The new x-ray method represents the formal analogy to powder patterns taken by neutron spectroscopy, such as by use of the time-of-flight method (*6*). Powder diffraction spectrography should be applicable in instances in which some resolution can be sacrificed for great reduction in exposure time.

BILL C. GIESSEN
Department of Metallurgy and Material Science, Massachusetts Institute of Technology, Cambridge 02139
GLEN E. GORDON
Department of Chemistry and
Laboratory for Nuclear Science, Massachusetts Institute of Technology

References and Notes

1. R. W. James, *The Optical Principles of the Diffraction of X-rays* (Bell, London, 1962), p. 6.
2. B. C. Giessen, in *Proc. Sagamore Army Materials Res. Conf. 12th*, J. J. Burke, N. L. Reed, V. Weiss, Eds. (Syracuse Univ. Press, Syracuse, N.Y., 1966), p. 273; ———, M. Morris, N. J. Grant, *Trans. Met. Soc. AIME* **239**, 883 (1967); P. Duwez, *Progr. Solid State Chem.* **3**, 377 (1966).
3. H. R. Bowman, E. K. Hyde, S. G. Thompson, R. C. Jared, *Science* **151**, 562 (1966).
4. Technical Measurement Corp., North Haven, Conn.
5. *International Tables for X-ray Crystallography* (Kynoch Press, Birmingham, England, 1962), vol. 3, p. 281.
6. R. M. Brugger, in *Thermal Neutron Scattering*, P. A. Egelstaff, Ed. (Academic Press, London, 1965), p. 53.
7. Aided by the AEC [contract AT(30-1) 905] and by the U.S. Army Research Office, Durham, N.C. (contract DA 31-124-ARO-D). We thank William Zoller for help and Robert Ogilvie and Roy Kaplow for lending equipment.

30 November 1967

Cavitation in Liquids Demonstrated by Ultrashort-Exposure Radiography

Abstract. *Using a field-emission x-ray tube, giving a much shorter pulse of rays than does conventional apparatus, we have demonstrated around a water jet the presence of a toroidal cavity that could not be detected visually. One advantage of this method of demonstrating cavitation is that it may be used with fluids and vessels that are opaque to light.*

For experimental purposes the presence of cavitation in a liquid is usually detected visually in specially prepared models. Occasionally, ultrasound-reflection and sound-detection devices are employed, but these merely indicate the occurrence of cavitation and do not demonstrate the extent and distribution of the phenomenon. For visual detection, abundant light is required (*1*), which enables direct observation or cinephotography in clear fluids. In